Supporting Information for

Sulfate-based Anionic Diblock Copolymer Nanoparticles for Efficient Occlusion within Zinc Oxide

Y. Ning, L. A. Fielding, T. S. Andrews, D. J. Growney, S. P. Armes*

Department of Chemistry, University of Sheffield, Brook Hill, Sheffield, South Yorkshire, S3 7HF, UK.

* Author to whom correspondence should be addressed (S.P.Armes@sheffield.ac.uk).

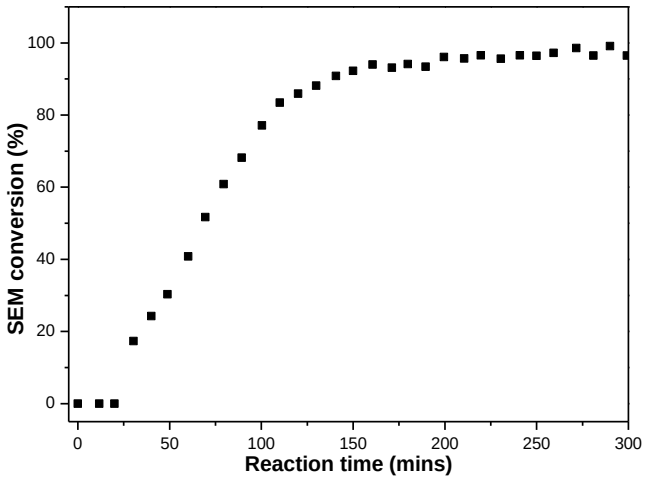

Figure S1. Conversion *vs* time curve calculated from ^{1}H NMR spectra (D_2O) for the RAFT synthesis of PSEM macro-CTA in water at 70 °C (target DP = 60; CTA/initiator molar ratio = 5.0).

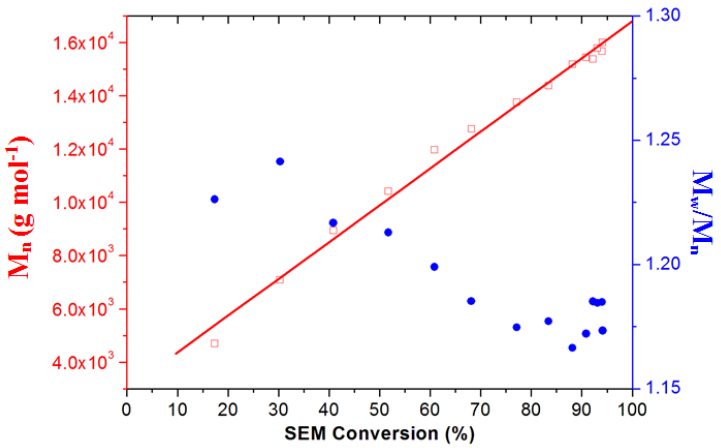

Figure S2. Evolution of the number-average molecular weight M_n (calculated using PEO standards) and polydispersity (M_w/M_n) of PSEM macro-CTA (target DP = 60; CTA/initiator molar ratio = 5.0) with monomer conversion as judged by aqueous GPC.

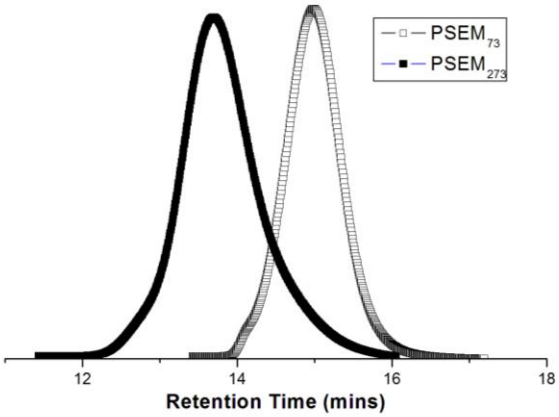

Figure S3. Aqueous GPC curves demonstrating the successful chain extension of $PSEM_{73}$ using SEM monomer. This 'self-blocking' experiment was conducted in aqueous solution at 70 °C using ACVA initiator ($PSEM_{73}$ macro-CTA/ACVA molar ratio = 5.0). This demonstrates high blocking efficiency for this $PSEM_{73}$ macro-CTA, which implies high RAFT chain-end fidelity.

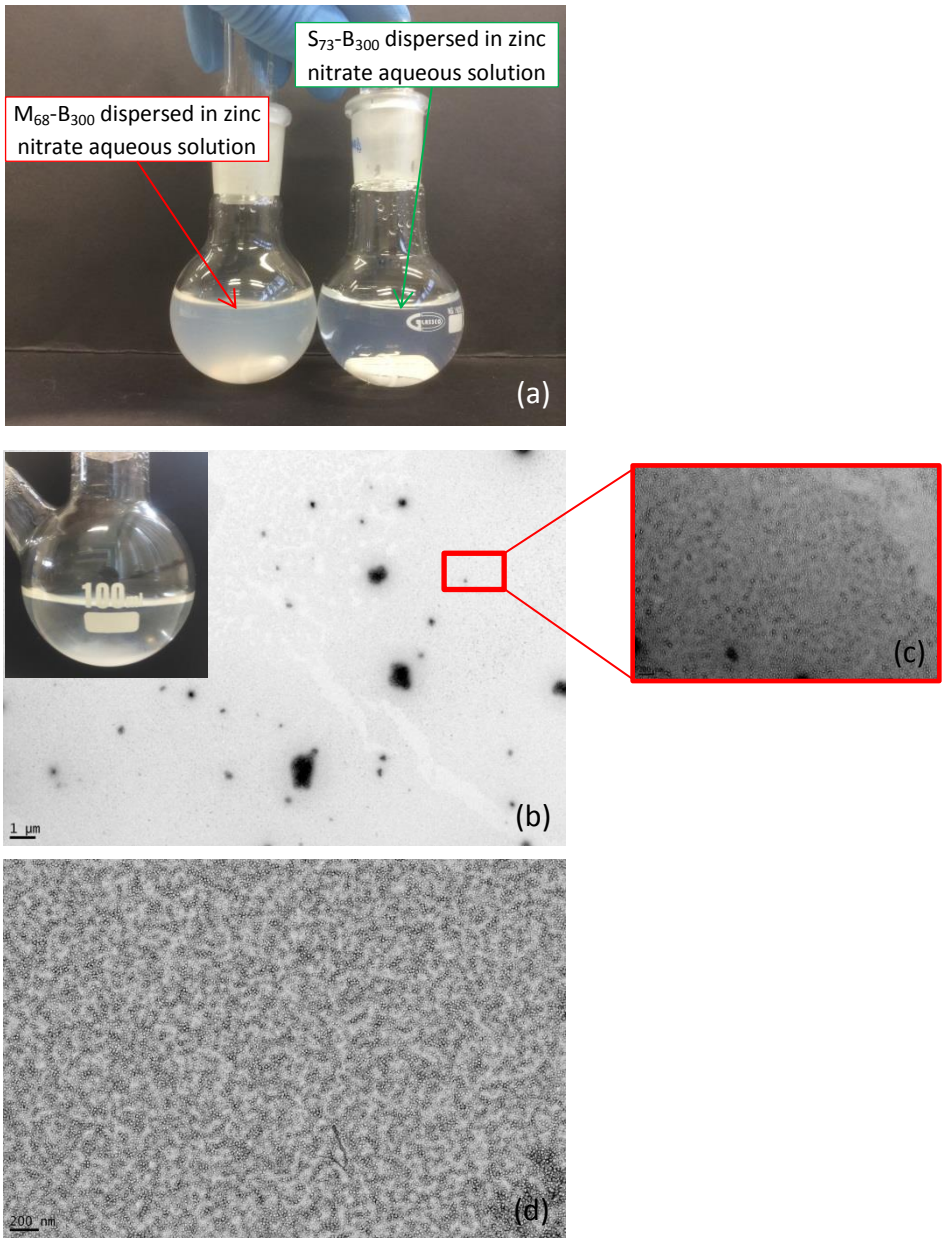

Figure S4. (a) Digital photograph recorded for 0.50 g dm^{-3} M_{68}-B_{300} and 0.50 g dm^{-3} S_{73}-B_{300} dispersed in aqueous zinc nitrate solution; (b) TEM images obtained for 0.50 g dm^{-3} S_{32}-B_{300} nanoparticles dispersed in aqueous zinc nitrate solution (inset shows the corresponding digital photograph); (c) magnified image of the area shown in image (b); (d) TEM images of 0.50 g dm^{-3} S_{73}-B_{300} nanoparticles dispersed in aqueous zinc nitrate solution. A white precipitate was formed immediately on addition of S_{32}-B_{300}, but a stable homogeneous aqueous dispersion is maintained for long time periods (months) in the presence of S_{73}-B_{300} nanoparticles.

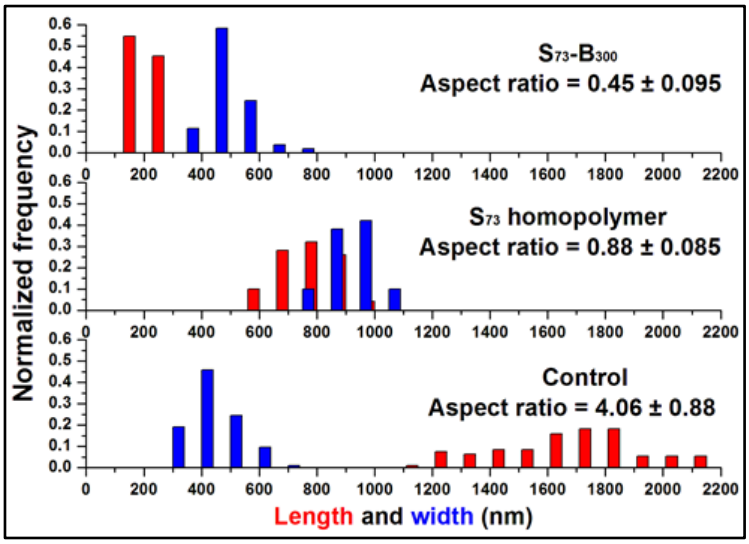

Figure S5. Histograms of the length and width comparison for the samples prepared in the absence of any additive (Control), S_{73} homopolymer, and S_{73}-B_{300} nanoparticle.

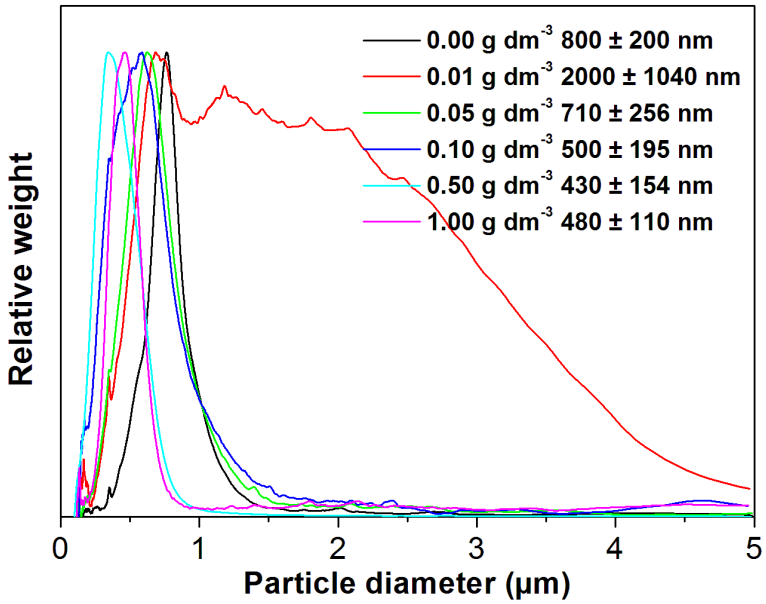

Figure S6. Weight-average particle diameters obtained for ZnO particles prepared in the presence of various concentrations of S_{73}-B_{300} copolymer nanoparticles, as determined by disk centrifuge photosedimentometry.

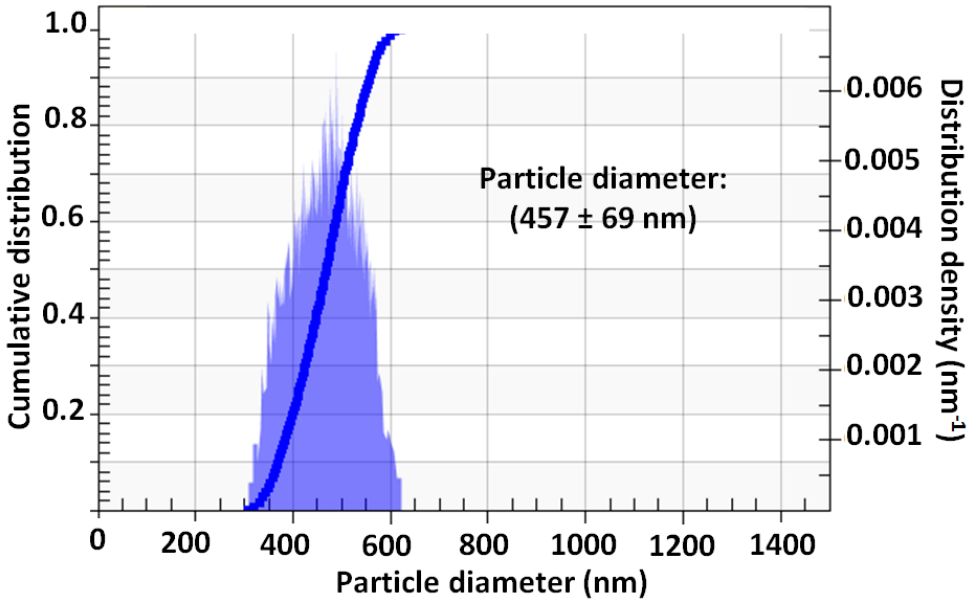

Figure S7. Volume-average particle size distribution determined for the S_{73}-B_{300}/ZnO nanocomposite before calcination, as determined by analytical centrifugation (LUMiSizer® instrument).

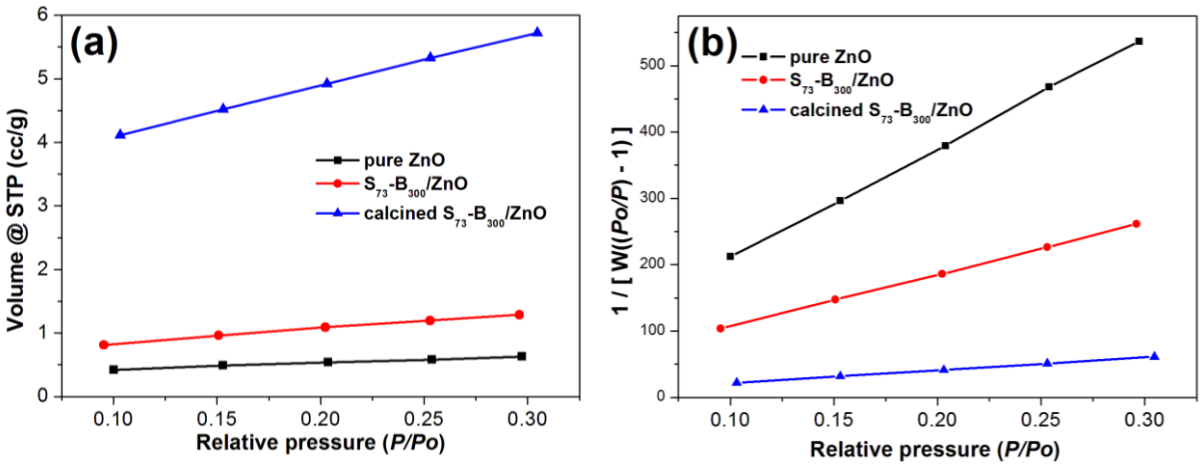

Figure S8. (a) Adsorbed volume of N_2 gas versus relative pressure (P/P_o) ranging from 0.10 to 0.30; (b) Linear BET plots of $1/[(W(P_o/P)-1)]$ versus *P/Po* ranging from 0.10 to 0.30.

The BET surface area of the pure ZnO, S_{73}-B_{300}/ZnO and calcined S_{73}-B_{300}/ZnO was calculated by N_2 adsorption (Nova 1000e instrument, Quantachrome). All samples were degassed at 40 °C overnight prior to measurements. The specific surface area (in $m^2\ g^{-1}$) was determined using the five-point BET method over a relative pressure (P/P_0) range of 0.10–0.30.

Table S1. Comparison of copolymer contents determined from TGA and carbon microanalyses.

	wt. %	vol. %
TGA	**23**	**56**
Carbon microanalysis	**25**	**58**